Midwave infrared InAs/GaSb superIattice photodiode with a dopant-free p-n junction.

*M. Delmas[1,2], J.B. Rodriguez[1,2], R. Taalat [1,2], L. Konczewicz[3,4], W. Desrat[3,4], S.Contreras[3,4], E. Giard[5], I. Ribet-Mohamed[5], P. Christol[1,2]**

[1]*Univ. Montpellier, IES, UMR 5214, F- 34000, Montpellier, France*

[2]*CNRS, IES, UMR 5214, F- 34000, Montpellier, France*

[3]*Univ. Montpellier, L2C, UMR 5221, F- 34000, Montpellier, France*

[4]*CNRS, L2C, UMR 5221, F- 34000, Montpellier, France*

[5]*ONERA, Chemin de la Hunière, F-91761, Palaiseau, France*

Abstract

Midwave infrared (MWIR) InAs/GaSb superlattice (SL) photodiode with a dopant-free p-n junction was fabricated by molecular beam epitaxy on GaSb substrate. Depending on the thickness ratio between InAs and GaSb layers in the SL period, the residual background carriers of this adjustable material can be either n-type or p-type. Using this flexibility in residual doping of the SL material, the p-n junction of the device is made with different non-intentionally doped (nid) SL structures. The SL photodiode processed shows a cut-off wavelength at 4.65µm at 77K, residual carrier concentration equal to $1.75x10^{15}$ cm^{-3}, dark current density as low as $2.8x10^{-8}A/cm^2$ at 50 mV reverse bias and R_0A product as high as $2x10^6\Omega.cm^2$. The results obtained demonstrate the possibility to fabricate a SL pin photodiode without intentional doping the pn junction.

Highlights :

- MWIR SL photodiode was made using the flexibility properties of InAs/GaSb Superlattice

- MWIR SL photodiode was made without intentional doping the pn junction

- Electrical and electro-optical characterizations of MWIR pin SL photodiode made of dopant-free p-n junction have been reported

PACS 72.40+w, 73.40.Kp, 73.61.Ey

Keywords : InAs/GaSb Superlattice, photodiode, dark current, midwave infrared

*Corresponding author: Tel.: (+33) 467 524 368; Fax: (+33) 467 544 842
e-mail address: christol@ies.univ-montp2.fr

1. Introduction

Twenty years ago, Yang and Bennet reported the first fabrication of Type-II InAs/GaSb superlattice (SL) pin photodiode operating in the midwave infrared (MWIR) [1]. Since then, many advances have been made, making the SL photodetector technology suitable for high performance infrared imaging [2]. In particular, important developments have been made to control the SL technology leading to a dual-color MWIR camera [3] and to raise the operating temperature of MWIR SL photodiode and focal plane arrays (FPAs) with demonstration of human body imaging up to 170K [4].

Despite these impressive progresses, experimental results on SL detectors have not yet reached their theoretical performances that are strongly dependent to their residual background carrier concentration. Consequently, fundamental studies on MWIR SL material, such as minority carrier lifetime [5-7], in plane and vertical effective masses [8] and mobilities [9, 10], residual background carrier concentration [11-13], have been investigated for a better understanding of the carrier transport in this minority carrier detector. Recently, influence of the SL period thickness and composition on the electrical and optical properties of MWIR SL photodetectors has been reported [14].

The non-intentionally doped (nid) active region of MWIR pin SL photodiode, fabricated by molecular beam epitaxy (MBE), usually exhibits a residual background carrier concentration between $5x10^{14}$ cm^{-3} and $5x10^{15}$ cm^{-3}. These values, in many cases extracted from capacitance-voltage (C-V) measurements [14-18], are related to the thickness and composition of the InAs/GaSb SL period. The type of conductivity of the nid region is also linked to the InAs/GaSb SL period. Indeed, because the nid GaSb and InAs layers have p-type and n-type residual backgrounds, respectively, the background of the nid SL active region is likely to be either n-type or p-type. The InAs/GaSb SL tends to result in n-type material for thicker InAs layer ("InAs-rich" structure) whereas thicker GaSb layer ("GaSb-rich" structure)

makes the material p-type [18]. Consequently, with this peculiar property of carrier-type flexiblity of SL material, it is possible to avoid doping the detector and fabricate a p-n junction by using only nid SL structures.

In this paper, we report on electrical and electro-optical characterizations of MWIR pin SL photodiode made of dopant-free p-n junction.

2. Choice and fabrication of the SL pin structure

The InAs/GaSb SL presents a specific staggered type-II (or type-III) band alignment, in which the top of the conduction band is below the bottom of the valence band. Consequently, the band gap of the SL periodic structure, determined by the energy difference between the first heavy hole state V1 and the first electron miniband C1, depends only on the layer thicknesses, in symmetric (same thickness of InAs and GaSb layers) or asymmetric (one of the two layers thicker than the other) configurations. To quantify the symmetric or asymmetric period design, we define the quantity R as the InAs to GaSb thickness ratio in each InAs/GaSb SL period. $R > 1$ corresponds to "InAs-rich" structure while $R < 1$ stands for "GaSb-rich" structure.

Calculations of miniband energies of SL structures have been performed using a modified envelope function approximation (EFA) model, sufficient to predict the band structure of MWIR SLs [19]. Fig. 1 reports the evolution of the calculated fundamental interminiband V1C1 energy transitions at 77K as a function of the SL period thickness, for different thickness ratio R. This figure highlights the possibilities of the SL structure to assign the 3-5µm MWIR spectral range. For a given band gap around 250 meV (λ_c = 5 µm) at 77K, we can choose different SL structures. One can be a symmetric InAs/GaSb SL structure (R=1) where the SL's period is composed by equal number of 10 InAs and GaSb monolayers (MLs). The others can be a n-type "InAs-rich" structure with R = 1.75, made of 7 MLs InAs / 4 MLs

GaSb per SL period or a p-type "GaSb-rich" structure (R = 0.5) with a SL period composed of 10 MLs InAs / 19 MLs GaSb.

Selected Symmetrical, "InAs-rich" and "GaSb-rich" structures were preliminary fabricated by MBE on GaSb substrate. Next, specific process with removing of the conductive GaSb substrate has been made [12] to perform Hall measurement as a function of temperature using magnetic field up to 1T. Temperature dependence of the effective carrier concentration n_H are presented in Fig. 2a and Fig. 2b. In the case of the symmetric SL structure (Fig. 2a), an apparent change in type of conductivity in the nid InAs/GaSb SL is observed around 120K. Because the MBE grown InAs layers are residual n-type while GaSb layers are residual p-type, the residual doping in symmetrical InAS/GaSb SL is therefore induced by the compensation, as a function of temperature, of donors in the InAs and acceptors in the GaSb layers. At low temperature, the sample is p-type with carrier density $p_H = 2.8 \times 10^{15}$ cm^{-3} at 77K. Such a change in type of conductivity is not observed in the case of nid "InAs-rich" and "GaSb-rich" SL samples (Fig 2b) that are, respectively, n-type and p-type in the whole range of temperature. At low temperature, the samples show carrier concentration equal to $8x10^{14}cm^{-3}$ for the n-type "InAs-rich" SL structure and $5x10^{15}$ cm^{-3} for the p-type "GaSb-rich" SL sample. These values are consistent with C-V measurements performed on diodes with similar SL designs [14].

Combining "InAs-rich" and "GaSb-rich" structures, the SL structure was grown by MBE on p-type GaSb (100) substrate. Fig. 3 shows the schematic view of the SL pin structure. The p-type absorbing layer was made of 1.5µm thick of nid "GaSb-rich" SL while the n-type layer was provided by a 200 nm thick of nid "InAs-rich" SL structure. Graded superlattice periods were used for avoiding any energy band offset between the "GaSb-rich" and the "InAs-rich" structures. For the same reason, several periods of doped "InAs-rich" and "GaSb-rich" SLs were inserted before the doped InAs and GaSb contact layers, respectively.

However, it is worth insisting on the fact that the p-n junction is located inside the nid part of the structure.

The crystalline quality and the SL period thicknesses were characterized using high resolution X-ray diffraction (HRXRD) measurements. As can be seen on the HRXRD spectrum shown in Fig. 4, the different SLs are lattice-matched to the GaSb substrate and each SL period can easily be identified.

The detector devices were then processed using standard optical photolithography techniques. CrAu was deposited as bottom and top contact metal. Mesa photodiodes were realized by wet etching using appropriate acids solution and polymerized photoresist was used to protect the etched surfaces from the ambient air [16]. The samples were wire bounded and packaged. Finally, the devices were placed in a LN2-cooled cryostat in order to perform photoresponse, capacitance-voltage (C-V) and current density voltage (J-V) measurements under dark conditions (0° field of view).

3. Characterization of the SL pin detector.

Photoresponse spectra of the dopant-free photodiode for different bias voltages at 80K were measured with a Fourier transform infrared (FTIR) spectrometer. The non-calibrated spectra, recorded in same conditions, are shown in Fig. 5. These spectra exhibits a cut-off wavelength at 4.65 µm with a bidimensional spectral shape which is a signature of "GaSb-rich" SL photodetector [14]. We observe also an increase of the photoresponse with reverse bias voltage. This behavior is probably due to an absorbing zone that would not be completely depleted. Increasing the reverse bias voltage would increase the depletion width, and thus would allow more carriers to be collected, leading to a enhancement of the photoresponse signal. To complete this analysis, spectral photoresponse measurements on samples with calibrated blackbody are planned.

Electrical measurements (J-V characteristics) performed in dark conditions at different operating temperatures, ranging from 77K to 225K, were measured using a Keithley 6517A electrometer to both apply the bias voltage and read the current delivered by the device. J-V curves are reported in Fig. 6a. Both in forward and reverse bias, these curves are the mark of a p-n junction. At 77K, dark current density of 2.8×10^{-8} A/cm^2 at a reverse bias of 50 mV was measured and R_0A product value equal to $2 \times 10^6 \Omega.cm^2$ was extracted at 0V. These values are among the best reported for SL MWIR photodiodes having a cut-off wavelength at 4.65µm at 77K [17]. In addition, the dark current density values extracted from J-V curves at a 50 mV reverse bias are reported as a function of reverse temperature (Arrhenius plot) in Fig. 6b. Temperature dependence of the dark-current density reveals that the dopant-free SL diode is diffusion-limited at high temperature, while it is Generation-Recombination (G-R) limited below 125K. This behavior is similar to that of "InAs-rich" MWIR pin diodes [14].

Additional C-V measurements at a frequency f = 1MHz were performed on diodes. Typical result at 77K is shown in Fig. 7 for a diode with a diameter of 310 µm. Residual carrier concentration $N_{res} = 1.75 \times 10^{15}$ cm^{-3} is extracted from the slope close to 0 V of the $(A/C)^2$ curves [17]. In agreement with behavior observed on photoresponse spectra under polarization, it is necessary to applied a reverse bias voltage over than 1.75 V to obtain the full depletion of the 1.5µm nid absorbing layer (inset of Fig. 7). From the C-V measurements, no information about the polarity of the carrier background in the nid region can be obtained but C-V characteristics are specific of p-n junction diodes.

4. Conclusion

A dopant-free p-n junction of a MWIR InAs/GaSb SL photodiode was fabricated. The p-n junction was made by using two different non-intentionally doped SL structures with p or n residual carrier concentration. Electrical characterizations performed on the SL device

confirmed the presence of a diode with results at the state of the art for InAs/GaSb SL photodetector having cut-off wavelength at 4.65 µm at 77K. Such result demonstrates the possibility to fabricate InAs/GaSb SL photodiode without intentional doping the active zone of the pin detector.

ACKNOWLEDGMENTS

This work is supported by the French DGA.

REFERENCES

[1] M.J. Yang, B.R. Bennet “InAs/GaSb infrared photovoltaic detector at 77K”, Electron. Lett. 30 (1994) 1710.

[2] A. Rogalski "Progress in focal plane array technologies", Prog. Quant. Electron. 36 (2012) 342

[3] F. Rutz, R. Rehm, M. Walther, J. Schmitz, L. Kirste, A. Wörl, J-M Masur, R. Scheibner, J. Ziegler, "InAs/GaSb superlattice technology" Inf. Phys Technol. 54 (2011) 237.

[4] M. Razeghi, S. Abdollahi Pour, E.K. Huang, G. Chen, A. Haddadi, B.M. Nguyen, "Type-II InAs/GaSb photodiodes and focal plane arrays aimed at high operating temperatures", Opto-Electron. Rev. 19 (2011) 261.

[5] S.P. Svensson, D. Donetsky, D. Wang, H. Hier, F.J. Crowne, G. Belenky, "Growth of type II strained layer superlattice, bulk InAs and GaSb materials for minority lifetime characterization", J. Crystal Growth 334 (2011) 103.

[6] L.M. Murray, K.S. Lokovic, B.V. Olson, A. Yildirim, T.F. Boggess, J.P. Prineas, "Effects of growth rate variations on carrier lifetime and interface structure in InAs/GaSb superlattices", J. Crystal Growth 386 (2014) 194.

[7] B. Klein, N. Gautam, E. Plis, T. Schuler-Sandy, T.J. Rotter, S. Krishna, B.C. Connely, G.D. Metcalfe, P. Shen, M. Wraback, "Carrier lifetime studies in midwave infrared type-II InAs/GaSb strained layer superlattice", J. Vac. Sci. Technol. B 32 (2014) 02C101.

[8] S. Suchalkin, G. Belenky, S.P. Svensson, B. Laikhtman, D. Smirnov, L.C. Tung, S. Bandara, "In plane and growth direction electron cyclotron effective mass in short period InAs/GaSb semiconductor superlattices", J. Appl. Phys. 110 (2011) 043720.

[9] S. Safa, A. Asgari, L. Faraone, "A study of vertical and in-plane electron mobility due to interface roughness scattering at low temperature in InAs/GaSb type-II superlattices", J. Appl. Phys. 114 (2013) 053712.

[10] F. Szmulowicz, G.J. Brown "Calculation of interface roughness scattering-limited vertical and horizontal mobilities in InAs/GaSb superlattices as a function of temperature", J. Appl. Phys. 113 (2013) 014302.

[11] H.J. Haugan, S. Elhamri, F. Szmulowicz, B. Ullrich, G.J. Brown, W.C. Mitchel, "Study of residual background carriers in midinfrared InAs/GaSb superlattices for uncooled detector operation", J. Appl. Phys. 92 (2008) 071102.

[12] C. Cervera, J. B. Rodriguez, J. P. Perez, H. Aït-Kaci, R. Chaghi, L. Konczewicz, S. Contreras, P. Christol, "Unambiguous determination of carrier concentration and mobility for InAs/GaSb superlattice photodiode optimization", J. Appl. Phys. 106 (2009) 033709.

[13] X. Guo, W. Ma, J. Huang, Y. Zhang, Y. Wei, K. Cui, Y. Cao, Q. Li, "Electrical properties of the absorber layer for mid, long and very long wavelength detection using type-II InAs/GaSb superlattice structures grown by molecular beam epitaxy", Semicond. Sci. Technol. 28 (2013) 045004.

[14] R. Taalat, J.B. Rodriguez, M. Delmas, P. Christol, "Influence of the period thickness and composition on the electro-optical properties of type-II InAs/GaSb midwave infrared superlattice photodetectors", J. Phys. D., 47 (2014) 015101.

[15] A. Hood, D. Hoffman, Y. Wei, F. Fuchs, M. Razeghi, "Capacitance-voltage investigation of high-purity InAs/GaSb superlattice photodiodes", Appl. Phys. Lett. 88 (2006) 052112.

[16] C. Cervera, J.B. Rodriguez, R. Chaghi, H. Aït-Kaci, P. Christol, "Characterization of midwave infrared InAs/GaSb superlattice photodiode" J. Appl. Phys 106 (2009) 024501.

[17] R. Taalat, J.B. Rodriguez, C. Cervera, I. Ribet-Mohamed, P. Christol, "Electrical characterizations of asymmetric InAs/GaSb superlattice MWIR photodiodes", Inf. Phys. Technol 59 (2013) 32

[18] G. Chen, A. M. Hoang, S. Bogdanov, A. Haddadi, P. R. Bijjam, B.-M. Nguyen, M. Razeghi, " Investigation of impurities in type-II InAs/GaSb superlattices via capacitance-voltage measurement", Appl. Phys. Lett. 103 (2013) 033512.

[19] J.B. Rodriguez, P. Christol, F. Chevrier, A. Joullié, "Optical characterization of symmetric InAs/GaSb superlattices for detection in the 3–5 mm spectral region," Physica E 28 (2005) 128

FIGURE CAPTIONS

Figure 1 : Calculated interminiband SL bandgap at 77K versus SL period thickness (1ML = 3Å) for different thickness ration R = InAs/GaSb.

Figure 2 : Measured apparent Hall carrier concentration N_H as a function of 1/T for the InAs/GaSb symmetrical SL structure (a) and for the "InAs-rich" and "GaSb-rich" SL structures (b).

Figure 3 : Schematic diagram of the SL p-n structure on p-type GaSb substrate with active zone made of nid SL stacking.

Figure 4 : High resolution X-ray diffraction scan of the SL structure lattice-matched to the GaSb substrate. Labels on satellite peaks identify the different InAs/GaSb SLs .

Figure 5: Non-calibrated spectral photoresponses of the InAs/GaSb SL photodiode at 80K for different bias voltages.

Figure 6 : Dark current density-voltage characteristics for different operating temperature from 77K to 225K (a). Arrhenius plot of the dark current density (-50mV). The diffusion and GR current regimes are reported (b).

Figure 7 : C-V measurements of the SL MWIR photodiode at 77K. In inset, plot of the square of A/C versus the reverse bias voltage, with A the area of the diode (diameter 310µm).

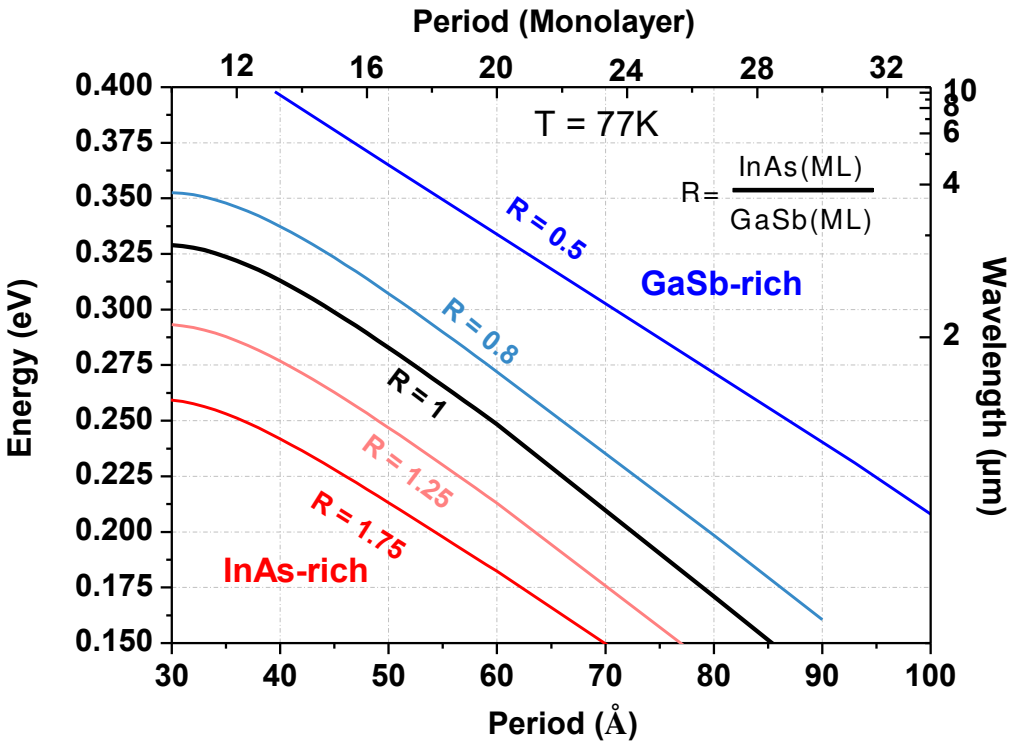

Figure 1

M. Delmas *et al.*

Midwave infrared InAs/GaSb superIattice photodiode with a dopant-free p-n junction.

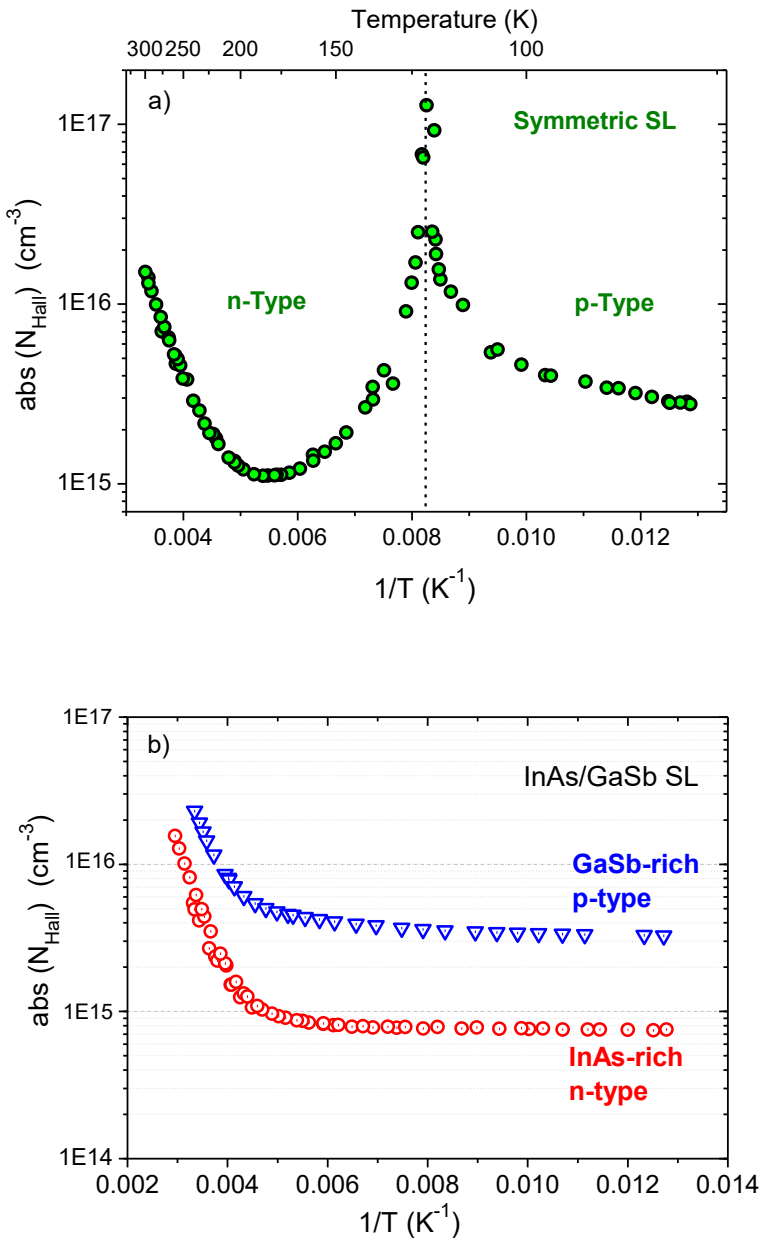

Figure 2

M. Delmas *et al.*

Midwave infrared InAs/GaSb superIattice photodiode with a dopant-free p-n junction.

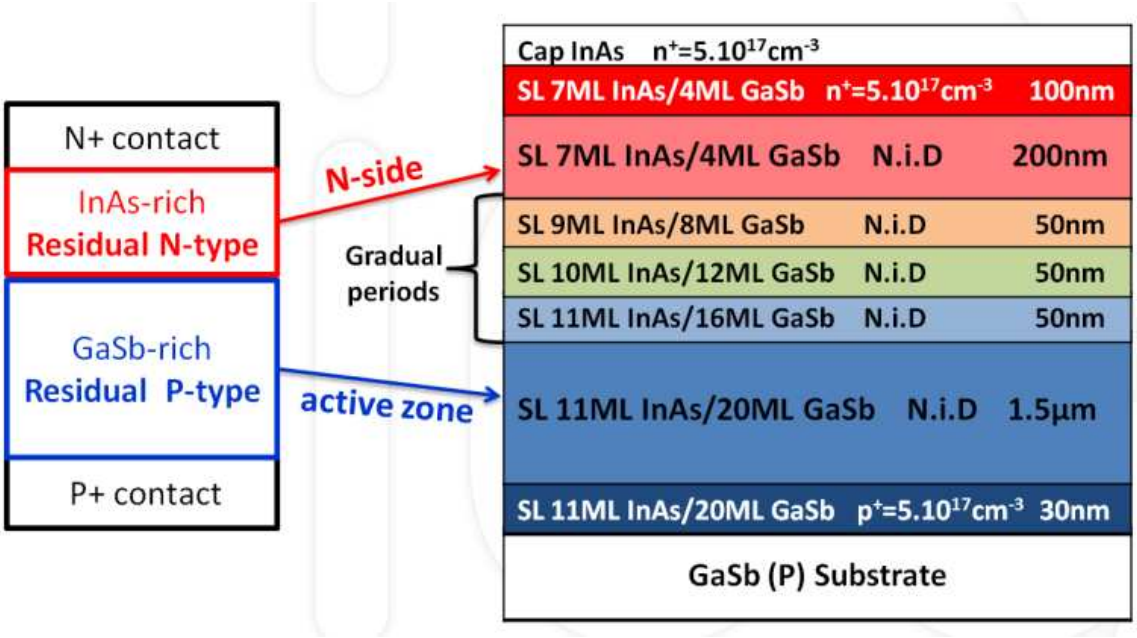

Figure 3

M. Delmas *et al.*

Midwave infrared InAs/GaSb superIattice photodiode with a dopant-free p-n junction.

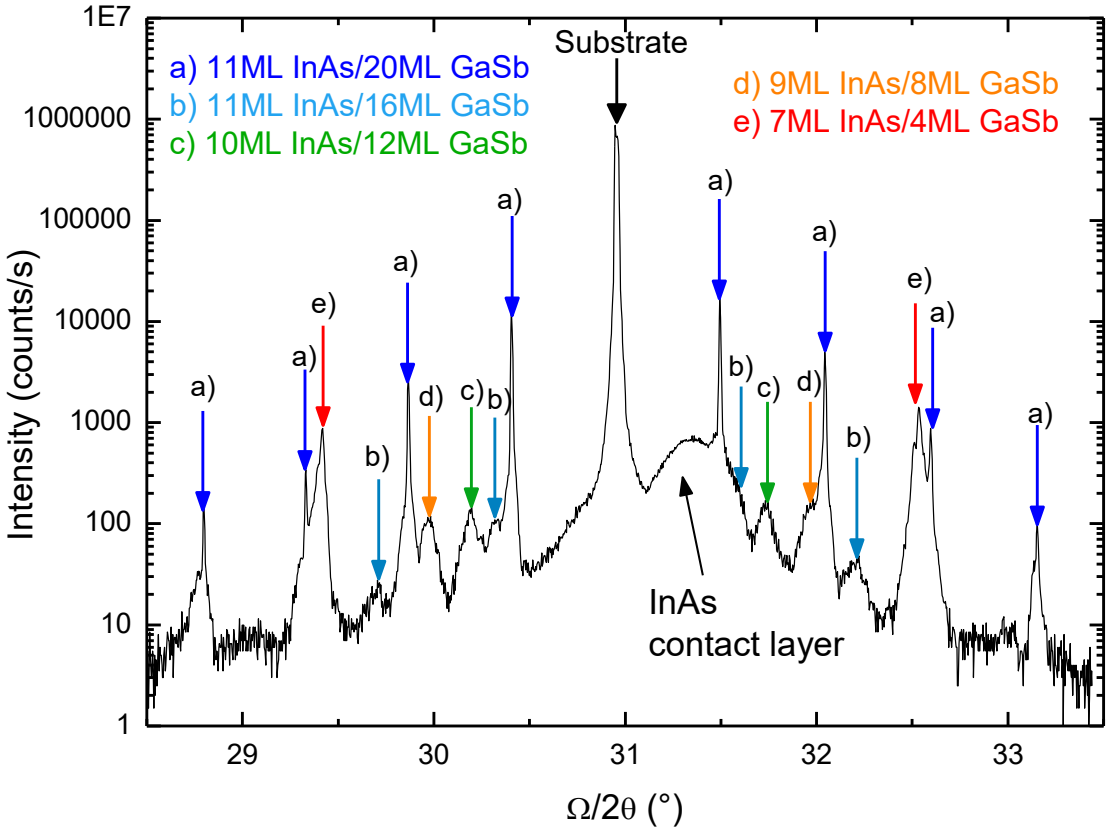

Figure 4

M. Delmas *et al.*

Midwave infrared InAs/GaSb superIattice photodiode with a dopant-free p-n junction.

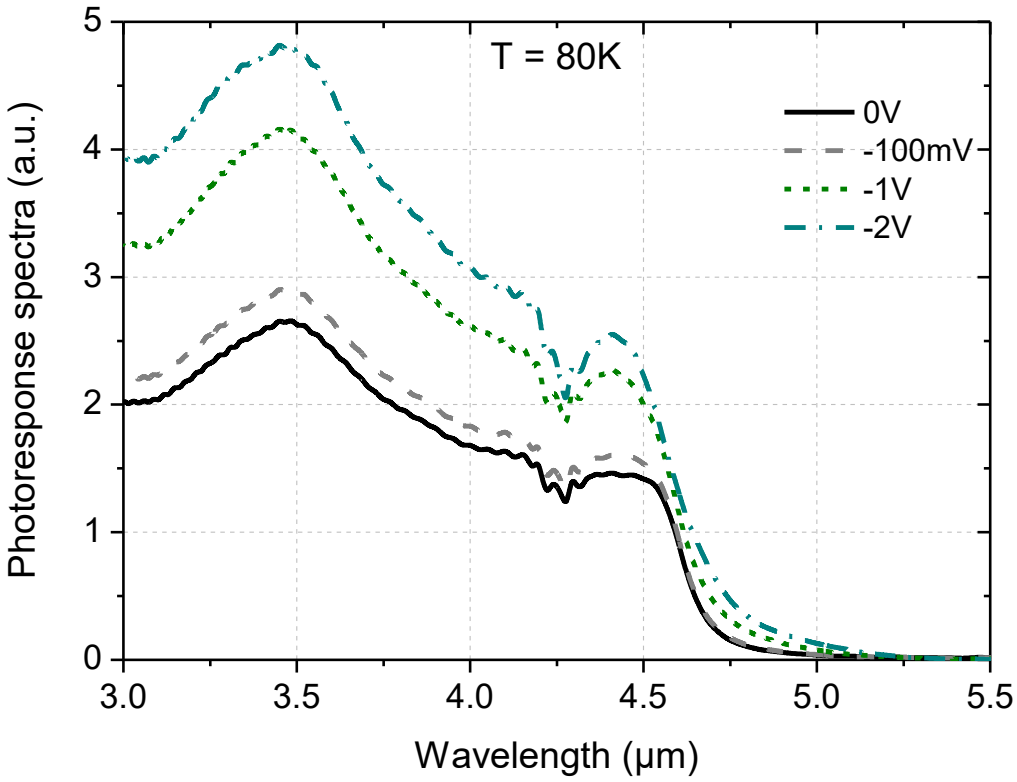

Figure 5

M. Delmas *et al.*

Midwave infrared InAs/GaSb superIattice photodiode with a dopant-free p-n junction.

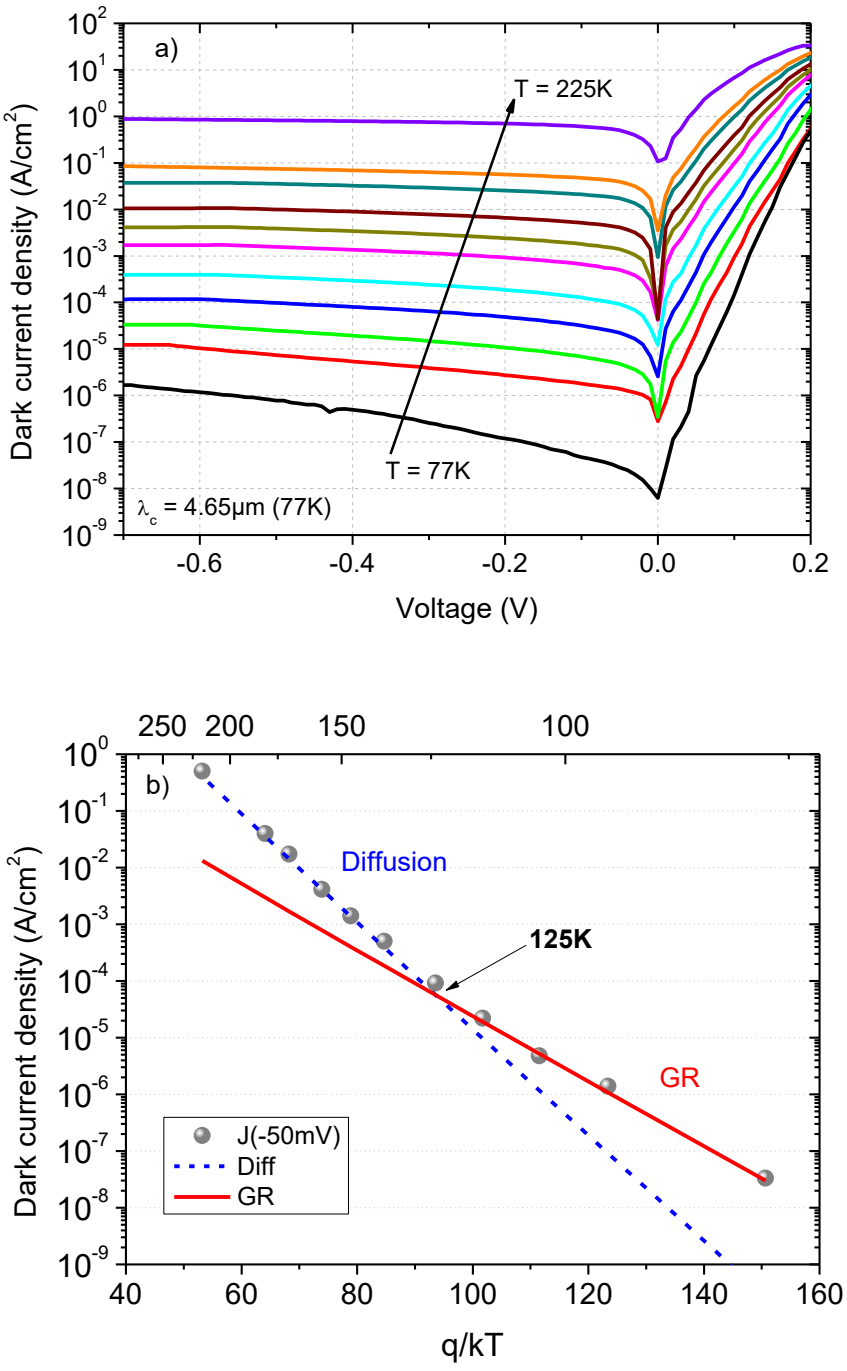

Figure 6

M. Delmas *et al.*

Midwave infrared InAs/GaSb superIattice photodiode with a dopant-free p-n junction.

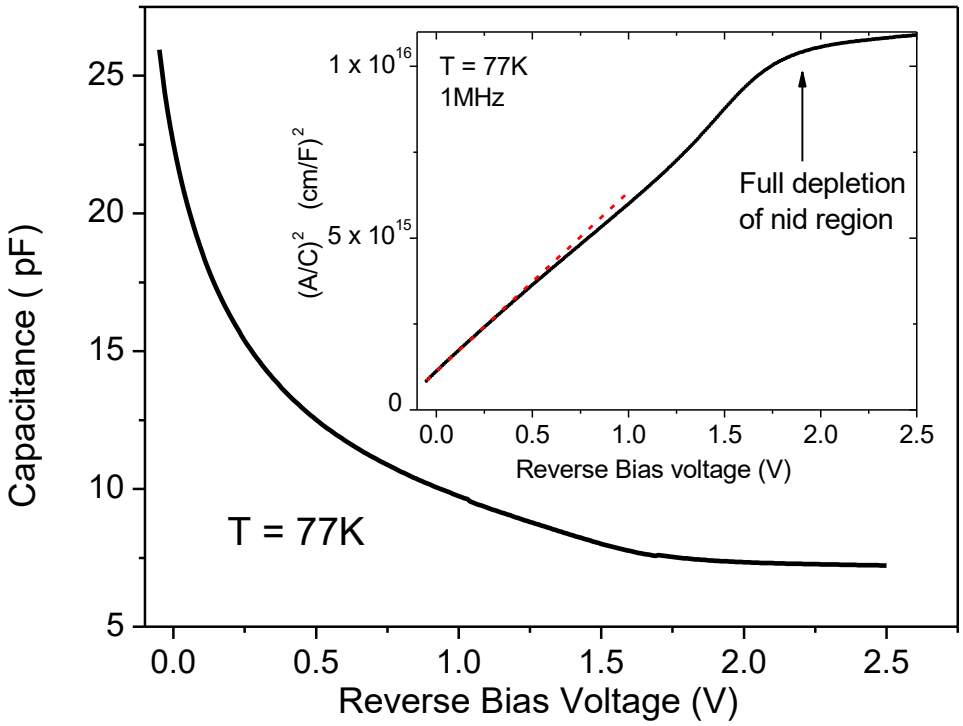

Figure 7

M. Delmas *et al.*

Midwave infrared InAs/GaSb superIattice photodiode with a dopant-free p-n junction.